



**HAL**  
open science

## Revealing the Nature of Black Pigments Used on Ancient Egyptian Papyri from Champollion Collection

Pierre-Olivier Autran, Catherine Dejoie, Pierre Bordet, Jean-Louis Hodeau, Caroline Dugand, Maeva Gervason, Michel Anne, Pauline Martinetto

### ► To cite this version:

Pierre-Olivier Autran, Catherine Dejoie, Pierre Bordet, Jean-Louis Hodeau, Caroline Dugand, et al.. Revealing the Nature of Black Pigments Used on Ancient Egyptian Papyri from Champollion Collection. *Analytical Chemistry*, 2021, 93 (2), pp.1135-1142. 10.1021/acs.analchem.0c04178 . hal-03363767v2

**HAL Id: hal-03363767**

**<https://hal.science/hal-03363767v2>**

Submitted on 7 Oct 2021

**HAL** is a multi-disciplinary open access archive for the deposit and dissemination of scientific research documents, whether they are published or not. The documents may come from teaching and research institutions in France or abroad, or from public or private research centers.

L'archive ouverte pluridisciplinaire **HAL**, est destinée au dépôt et à la diffusion de documents scientifiques de niveau recherche, publiés ou non, émanant des établissements d'enseignement et de recherche français ou étrangers, des laboratoires publics ou privés.

# Revealing the Nature of Black Pigments Used on Ancient Egyptian Papyri from Champollion Collection

Pierre-Olivier Autran,\* Catherine Dejoie, Pierre Bordet, Jean-Louis Hodeau, Caroline Dugand, Maeva Gervason, Michel Anne, and Pauline Martinetto\*

**ABSTRACT:** Although numerous papyri from ancient Egypt have been collected and preserved over the centuries, the recipe used to prepare black inks was only reported in manuscripts from the late Greco-Roman period. Black inks were mostly obtained after mixing carbon black with a binder agent and water. In previous studies performed on black inks apposed on papyri from ancient Egypt, additional chemical elements such as lead, iron, or copper were also identified, and the resulting chemical contrast with the papyrus support was used to virtually decrypt highly degraded or rolled papyri. Combining a series of synchrotron-based techniques with Raman spectroscopy and scanning electron microscopy, we investigated 10 papyri fragments from J.-F. Champollion's private collection. For each fragment, the carbon-black pigment found in the ink is identified as flame carbon (lampblack or soot). Using Xray diffraction computed tomography, we show that the diffraction signal of the carbon-based pigment itself can be isolated. As a result, a contrast with the papyrus support is obtained, even in the absence of a specific chemical element in the ink. This is opening up new opportunities to decipher words written millennia ago, as part of our Cultural Heritage.

## INTRODUCTION

The first attested black writings in ancient Egypt, dated from the fourth millennium BC, have been found on a series of gesso objects<sup>1</sup> from tomb group 1466 in the cemetery of Armant.<sup>2</sup> A few centuries later and for a few millennia, papyrus became the privileged support for the dissemination of information. Papyrus is an aquatic plant, naturally present in the Nile delta, and used after suitable preparation in several aspects of everyday life, such as ropes, sandals, or writing support.<sup>1</sup> Although numerous written and painted papyri from ancient Egypt were collected and preserved over the centuries to the best of our knowledge, none of them ever mentioned the recipe used by ancient Egyptians to prepare the black inks deposited on the papyrus.<sup>3</sup> The first written recipes were accounted for by Philo of Byzantium,<sup>4</sup> Discorides,<sup>5</sup> Pliny the Elder,<sup>6</sup> and Vitruvius<sup>7</sup> during the Greco-Roman period, with a description of pigment manufacturing processes and ingredients employed as writing material. Black inks in early times were generally depicted as a hydrated mixture of a binder agent (Arabic gum or animal glue) and of a carbon-based pigment, commonly flame carbon retrieved from the soot of burned oil, resin, fat, vegetals, or ground chars obtained from different wood essences. Later in history, black inks evolved from purely carbon inks to iron gall inks (iron salts mixed with tannic acids), mainly because of the increasing use of parchment as writing support, which requires higher adherence. A transition period where a mixed composition of both carbon and metallic salts (mainly iron or copper sulfates) was used was postulated<sup>8</sup> and is still under debate. Several studies were performed on black inks apposed on ancient papyri coming from different collections and covering a large period, from the Middle Kingdom to the Roman period. The object of these studies was not only to decipher the ink recipe but also to find a way to decrypt highly degraded or rolled papyri, for example, using a chemical contrast between the ink and the papyrus support. Analyses mainly rely on nondestructive techniques such as X-ray radiography<sup>9</sup> and Xray computed tomography<sup>10</sup> (CT), X-ray absorption spectroscopy<sup>11</sup> (XAS), X-ray fluorescence<sup>12</sup> (XRF), and Raman spectroscopy or Fourier transform infrared spectroscopy.<sup>13</sup> In most of these studies, chemical elements such as copper,<sup>11</sup> lead,<sup>10,14</sup> or iron<sup>15</sup> were found in the ink, offering a good chemical contrast compared to the raw papyrus support. Using such an approach, for the first time in centuries, the burned papyri of Herculaneum could be read again.<sup>10,14</sup> Nevertheless, the origin of the copper, lead, or iron, intentional addition or accidental contamination, is still unknown. Several hypotheses attempt to explain the presence of lead found in several collections from the Middle Kingdom to first century AD, with possibly an intentional addition of lead-based compounds in the binding medium as a drying agent, or the use of the black mineral galena, even if no definite answer has been accepted so far. Lead carboxylates were also identified in a few studies,<sup>9,16</sup> possibly resulting from the degradation of other

lead-based compounds. Concerning copper,<sup>11</sup> the authors assumed that the black pigment used for the ink was obtained from by-products of technical metallurgy, glass, and glaze production processes that were also used to produce carbon inks during the early centuries BCE. Finally, the presence of iron in a late papyrus from the 1st century CE has been linked to the use of iron gall inks.<sup>17</sup> The presence of all these elements – lead in particular – does not show any apparent correlation with a specific period, and the exact ink recipe or any evolution of it remains unclear. The main carbon-based pigment used to manufacture black inks in ancient Egypt is known to be carbon black, as reported by Lucas and Harris<sup>1</sup> and Nicholson and Shaw.<sup>18</sup> The terminology concerning historical carbon-based black pigments has evolved with time, and we chose to use the term flame carbon, as proposed by J. Winter.<sup>19</sup> Zerdoun<sup>3</sup> reports the use of flame carbon not only as pigment for inks but also for paint and varnishes, but with no additional detail concerning the way the pigment was identified. If the carbon nature of the black pigment can be easily verified using Raman spectroscopy,<sup>20</sup> the specific use of flame carbon instead of any other carbon-based pigments (e.g., obtained from the combustion of wood or fruit nuts) is more difficult to assess.<sup>21</sup> This difficulty is linked to the intrinsic nature of carbon-based pigments, no matter their origin: their chemical composition is similar (mainly exclusively carbon), and they all present an amorphous structure, making most chemical and structural techniques nonconclusive. In the absence of elements such as copper, lead, or iron in the ink, the possibility to use the carbon-based pigment itself as a contrasting agent to read damaged or unrolled manuscripts is an appealing alternative. Nevertheless, the presence of papyrus as support is making this alternative challenging. Indeed, the support is made of stacks of raw papyrus strips, characterized by a fibrous structure at the macroscopic scale.<sup>22</sup> The main constituent of papyrus is cellulose, a polysaccharide of chemical formula  $(C_6H_{10}O_5)_n$  with a semicrystalline crystallographic structure.<sup>22</sup> Considering the chemical similarities and the noncrystalline nature of both the carbon-based pigment and the papyrus support, neither XRF and XAS techniques nor X-ray diffraction (XRD) techniques seem to be suited for separating the pigment from papyrus contributions. In addition, the papyrus surface is highly heterogeneous (lack of flatness, presence of contaminating elements), and the amount of black pigment deposited is quite diluted. Combining CT and deep learning, a recent study has been carried out to read scrolled or burned papyri fragments<sup>23</sup> without using any chemical element as a contrasting agent, and the first results obtained on modern papyrus reproductions are promising. The object of the current study is to gain insight into black ink formulation in ancient Egypt, by investigating papyri fragments from J.-F. Champollion's private collection, curated by the Musée Champollion, Ise`re department, Vif, France. The collection contains a total of 280 fragments, the largest showing scenes belonging most probably from the Book of the Dead, with an estimated dating by Egyptologists to the New Kingdom period. These fragments have been preserved by the Champollion family for the last two centuries, and 10 of them have been selected for the current study (Figure 1). A series of synchrotron-based techniques have been implemented and combined with Raman spectroscopy and scanning electron microscopy. Here, we show that the carbon-based pigment used in the ink can be unequivocally identified as flame carbon. Moreover, using XRD computed tomography, the diffraction signal of the carbon-based pigment can be isolated, thus offering a contrast with the papyrus support in the absence of specific chemical elements in the ink.

## EXPERIMENTAL SECTION

Ten papyrus fragments, showing one or more black ink lines at their surface, were selected and kindly provided by the Champollion museum, Département de l'Isère, Vif, France (Figure 1). Among them, the PAP-6 fragment represents the god Ra, the deity of the sun, facing the hands, raised in adoration, of the supposed deceased. The PAP-7 fragment presents discernable black and red hieroglyphic writings, and the symbols "mouth," "reed," or "sedge" can be identified. Reference grape black pigment was obtained after the carbonization of dried vines. Carbonization was carried out in a muffle furnace (300 °C for 4 h). "Noir de fume`e" (flame carbon) (Dousselin) and peach black (Kremer Pigmente) references were purchased. Scanning electron microscopy (SEM) was carried out using a Zeiss Ultra+ microscope. Microanalysis (EDX) measurements were performed using a Silicon Drift (SDD) detector. Papyrus fragments were mounted in a homemade holder to prevent both sample contamination and charging effects (see the Supporting Information). Reference samples were spread on carbon adhesive. Raman spectroscopy was carried out using a 633 nm radiation wavelength on a WITec UHTS300 Raman spectrometer coupled with an iDus 401 CCD camera. All measurements were restrained to 1 mW power (20–60 s acquisition time per point) to avoid beam damage. All the spectra were fitted using the Origin v6.1 software package.

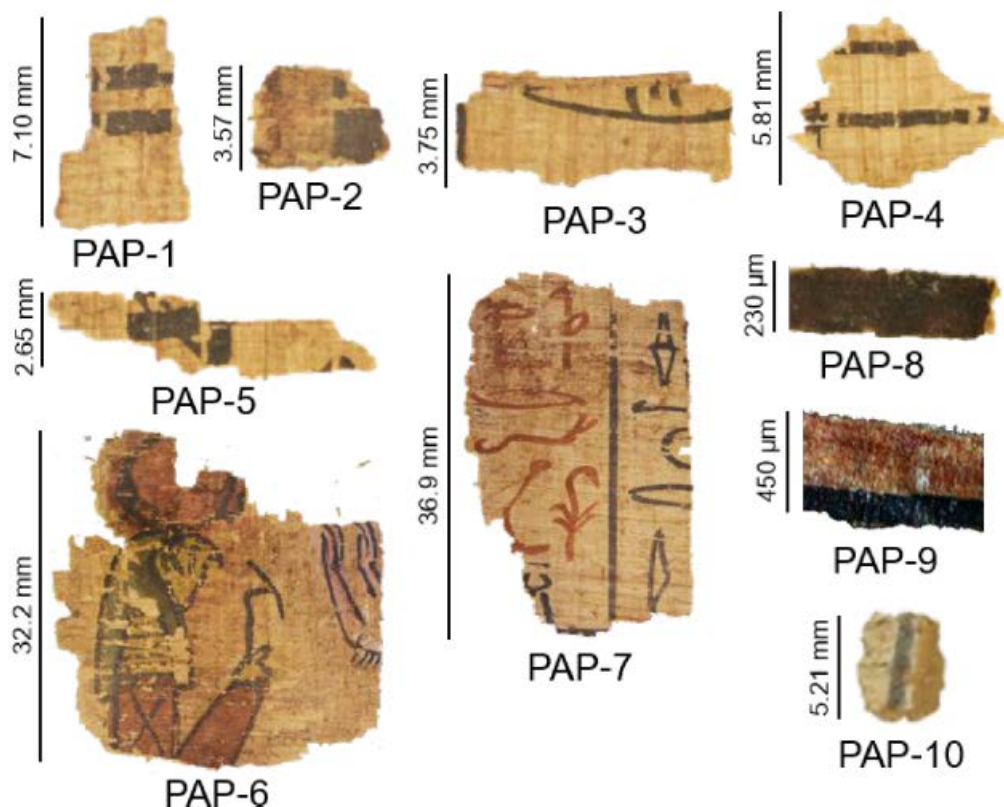


Figure 1. Papyrus fragments from the Champollion collection investigated in the current study (Champollion museum collection, Departement de l'Isere, Vif, France).

Synchrotron XRD and fluorescence (XRF) experiments were performed at the European Synchrotron Radiation Facility (ESRF, Grenoble, France) at the ID22 beamline. XRD data were collected using a Perkin Elmer XRD 1611CP3 detector, at a wavelength of  $0.4009 \text{ \AA}$  (31 keV) and with a beam size of  $1 \text{ mm} \times 0.1 \text{ mm}$  ( $h \times v$ ). The sample-detector distance was adjusted to 1400 mm. Both wavelength and detector parameters were calibrated using a pattern from a silicon NIST 640c standard. Fragments were held using dedicated 3D-printed frames (Figure S1). For all the samples, at each measurement point, 100 diffraction patterns (1 s per pattern) were collected, before averaging to improve the overall statistics. One-dimensional diffraction patterns were retrieved using the PyFAI<sup>24</sup> library. Refinements were carried out using the TOPAS software.<sup>25</sup> X-ray fluorescence spectra were recorded with a beam of  $100 \times 100 \mu\text{m}^2$  using a Hitachi Vortex 90EX SDD. Processing was done using the PyMca<sup>26</sup> software. X-ray diffraction (XRD-CT) and fluorescence (XRF-CT) computed tomography<sup>27,28</sup> experiments were carried out at the ID11 beamline at the ESRF, using a  $2 \times 2 \mu\text{m}^2$  X-ray beam and a wavelength of  $0.1897 \text{ \AA}$  (65 keV). Diffraction data were collected using a FReLoN 4 M CCD camera positioned at 10 cm from the sample. Experimental parameters were calibrated using a diffraction pattern collected on a reference ceria sample. XRF data were recorded using an energy dispersive X-ray detector (SGX Sensortech, SiriusSD). Papyrus samples were mounted on Mitegen microgrids, and data were recorded by scanning the sample keeping fixed rotation angles; 180 rotations were achieved, collecting both XRD and XRF data simultaneously (1 s per measurement point). The procedure to reconstruct the slices is detailed in the [Supporting Information](#).

## RESULTS AND DISCUSSION

**Blank Papyrus.** Both surface and bulk morphologies of the ancient papyrus supports were investigated combining SEM, XRF-CT, and XRD-CT. As mentioned in the Introduction, the support is made of stacks of papyrus strips, hammered and pressed together before polishing,<sup>18</sup> and the resulting orthogonal pattern with fibers running horizontally and vertically is still clearly visible on most of the fragments (e.g., PAP-4 in

Figure 1). The surface of the papyrus support shows heterogeneity, with grains disseminated all over (Figure 2A). During the manufacturing process, papyrus strips could be either cut off or peeled down from the plant pith, and Wallert has shown that these two preparation methods could be identified by SEM on freshly prepared papyrus.<sup>29</sup> Nevertheless, the unevenness of the surface resulting from the peeling method tends to disappear after polishing and drying of the papyrus, making our observations nonconclusive. The bulk morphology of the papyrus support was retrieved on PAP-8 and PAP-9 using XRF-CT and XRD-CT (Figure 3). The section of two parenchymal cells can be seen for PAP-9, sandwiched into two walls, probably made of similar tube-like parenchymal cells running parallel to the slice. The flattened oval shape of the cells is compatible with a phase of hammering during the manufacturing process, as mentioned in earlier works.<sup>18</sup> Similar features are seen for PAP-8, with the section of one parenchymal cell visible. The elemental composition of each fragment, retrieved by XRF, is given in Table S1. By performing complementary EDX analyses, we saw that chemical elements such as calcium (Ca), potassium (K), manganese (Mn), silicon (Si), and sodium (Na) were found in most of the samples. These elements were proved to be part of the plant growth,<sup>22</sup> and their respective concentrations vary depending on the growing locations of the papyrus.<sup>30</sup> In addition to these, iron (Fe), lead (Pb), and tin (Sn) were also detected. These latter elements exclusively appear as micrometer-sized clusters at the surface of the papyrus fragments, as revealed by two-dimensional (Figure 2A) and three-dimensional (Figure 3A,D) chemical mapping. Although these surface clusters may result from contamination introduced by the hammering and polishing process of the papyrus support in ancient times, later pollution from the environment or storing process may also be the cause. A diffraction pattern measured on a blank zone of PAP-1 is shown in Figure 2B. Three main phases were identified, and a Rietveld refinement was tentatively performed. The pattern is dominated by cellulose, the major component of papyrus. Some features on the main peaks of cellulose may indicate the presence of two cellulosic phases of varying crystallinity (both based on cellulose I $\beta$  structure), possibly resulting from an aging process, and this will be discussed in a further communication. In addition to cellulose, two hydrated calcium oxalate phases, weddellite and whewellite, were included in the fit. The presence of these two phases results from the reaction between the oxalic acid present in fast-growing plants (e.g., papyrus) with calcium extracted by the plant from the soil.<sup>22</sup> A number of diffraction peaks present in the diffraction pattern could not be indexed. If quartz, explained by the presence of sand in the environment,<sup>15</sup> or calcite were found in some other diffraction patterns, no crystalline phases in relation to the Sn, Pb, or As elements were identified. This may be explained by the random presence of these grains at the surface of the papyrus, their small amount, possibly their noncrystalline nature, or, as shown by the presence of nonindexed peaks in the diffraction pattern displayed in Figure 2B, the absence of the relevant structures in the powder diffraction databases we consulted (PDF2 2003 and PDF4+ 2019).<sup>31</sup>

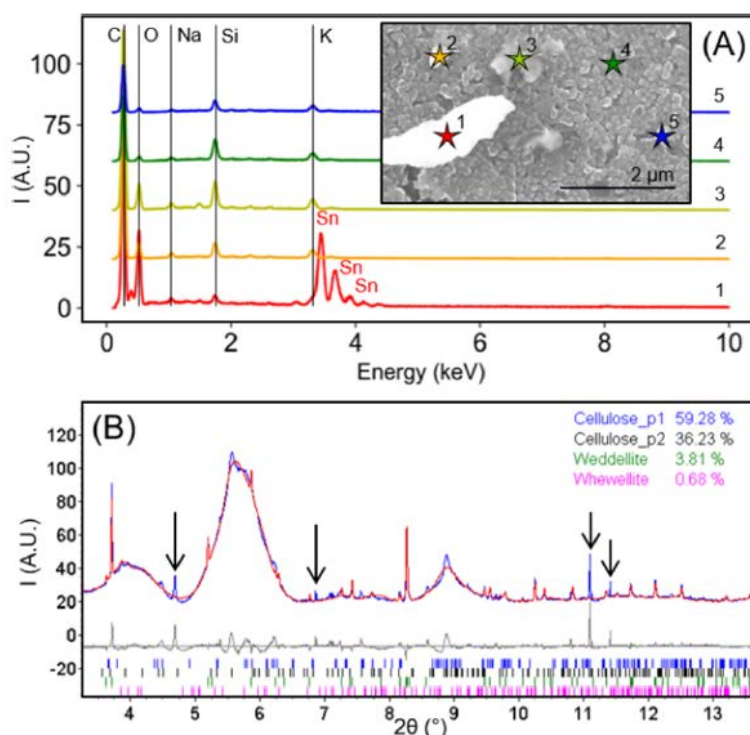




Figure 2. (A) EDX spectra recorded at five different positions at the surface of PAP-1, with corresponding SEM backscattering image (20 kV, WD = 8.2 mm) in the insert. A Sn cluster was identified. (B) Rietveld refinement of a powder diffraction pattern recorded on the papyrus support of PAP-1 ( $\lambda = 0.4009 \text{ \AA}$ ). The  $I\beta$  structural model was used for both Cellulose\_p1 and Cellulose\_p2 (blue: experimental data, red: calculated pattern, gray: difference curve). Black arrows indicate nonindexed diffraction peaks.

**Ink Composition.** The carbon-based nature of the black pigment of the ink was confirmed by Raman spectroscopy, and a spectrum collected on fragment PAP-6 is displayed in Figure 4A. The two bands pointing at  $1338$  and  $1593 \text{ cm}^{-1}$  were immediately correlated to the ink, as blank papyrus did not show any particular Raman signal in this wavenumber domain. Carbonaceous materials show preeminent features in the  $1000\text{--}1800 \text{ cm}^{-1}$  region depending on their degree of disorder and crystallinity.<sup>32</sup> In crystalline graphite, a narrow band around  $1580 \text{ cm}^{-1}$ , the G band, corresponds to the in-plane stretching vibrational mode of  $sp^2$  carbons in aromatic rings, with  $E_{2g}$  symmetry.<sup>33</sup> When the disorder of  $sp^2$  carbons increases, the G band broadens, and new bands, called D bands, appear, resulting in a larger band centered at  $\sim 1340 \text{ cm}^{-1}$ . Both G and D bands were identified on the Raman spectra collected on the black ink of our papyrus fragments (Figure 4A), in agreement with the use of a carbon-based pigment in an amorphous state. It has been shown that spectral parameters such as the position of the G and D bands, their width, and intensities can be used to discriminate between several kinds of carbon-based pigments<sup>21,34</sup> and to retrieve the age of the writings<sup>35</sup> on ancient papyrus. All the spectra collected on our papyrus fragments were fitted using a two-band model (Table S2). The fit obtained from a spectrum collected on the black scepter of Ra (PAP-6) is shown in Figure S2. Assessment of the background proved to be difficult, with a strong and variable fluorescence arising from the papyrus support. Because of this, intensities of the G and D bands, poorly trustable, were not extracted. The width of the G band as a function of the position is plotted in Figure 4. Data points corresponding to three carbonbased reference pigments (peach black, grape black, and flame carbon) are also shown. Data points retrieved from the same

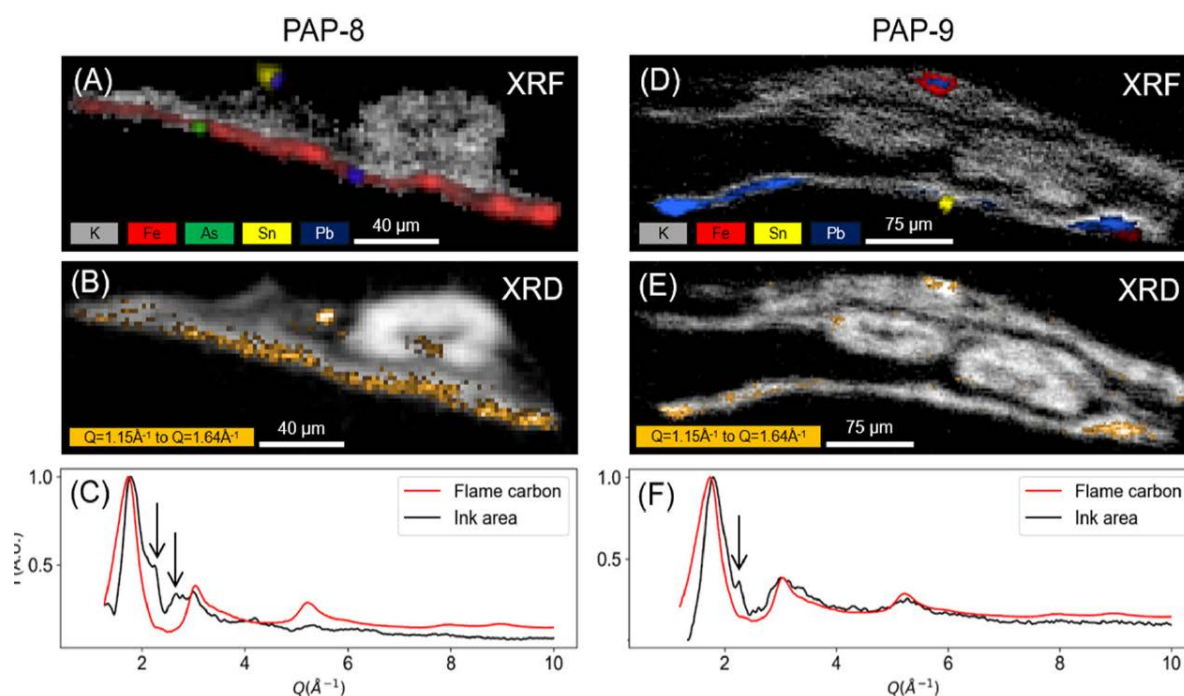


Figure 3. XRF-CT and XRD-CT reconstructed slices of PAP-8 and PAP-9. (A) and (D) XRF-CT of PAP-8 and PAP-9 papyrus fragment, respectively. Iron signal and lead signal match the inked surface of the papyrus of PAP-8 and PAP-9, respectively. (B) and (E) XRD-CT of PAP-8 and PAP-9, respectively. The white color represents the summed diffraction signal and the orange color the contribution of the signal between  $Q = 1.15$  and  $1.64 \text{ \AA}^{-1}$  (flame carbon diffraction peak position). The contrast, in relation to the presence of the carbon-based pigment in the ink, is obtained only after the subtraction of the average signal. Orange dots found away from the pigment signal correspond to undetermined crystalline phases. (C) and (F) XRD-CT reverse analysis after subtraction of an averaged signal of the blank papyrus, from the ink areas highlighted in orange in (B) and (E), respectively. The XRD pattern of a flame carbon standard is given for comparison. The black arrows indicate diffraction peaks from additional unidentified crystalline phases.

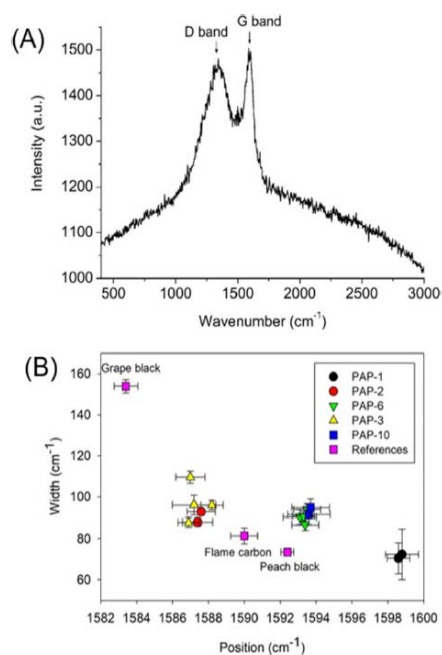


Figure 4. (A) Raman spectrum recorded on the black sceptor of Ra (PAP-6). (B) Width as a function of position for the G band.

papyrus fragment tend to form homogeneous groups. This clustering could be a way to identify which fragment from the Champollion collection may belong to the same papyrus. On the other hand, comparison to the reference data points does not bring any further information to clarify the origin of the carbon-based pigment. Concerning the spectral parameters of the D band (Figure S2), higher dispersion of the data is observed, the fit of this broader band being more influenced by any background fluctuation. The morphology of the carbon-based pigment was investigated using SEM, and a picture obtained for PAP-2 is shown in Figure 5A. The same overall morphology has been found for all the fragments: spheroidal particles of about 85 nm (+/- 10 nm) in diameter. The SEM pictures obtained from our three reference pigments, flame carbon, peach black, and grape black are shown in Figure 5B and Figure S3A,B, respectively, each of them showing a specific morphology. The flame carbon reference is characterized by spherical particles of about 170 nm in size with smooth surfaces, as expected for such a kind of carbon-based pigment.<sup>19,36</sup> Knowing that the size of flame carbon particles may vary from 80 to 200 nm,<sup>19,36</sup> the carbon-based pigment found in the ink of ancient papyrus from the Champollion collection is attributed to flame carbon. The ink deposited on Champollion papyrus was further investigated using XRF, and for each fragment, the elemental composition of the ink was compared with the one obtained from the papyrus support (Table S1). We mainly focused on three elements, copper, iron, and lead, as these have been reported by several authors in earlier studies.<sup>9-14</sup> No contrast between the ink and the blank papyrus was revealed when using copper as a discriminating element. On the other hand, a larger amount of lead was found in the ink of PAP-7 and PAP-9 (Table S1), and indeed for these two fragments, a contrast is visible on corresponding chemical maps (Figures 3D and 6). Both the arm garment decoration on PAP-6 and the shape of the mouth hieroglyph of PAP-7 are distinguishable from the surrounding. However, in the case of PAP-6, the contrast is present only in the four black stripes of the garment and does not appear on the black line delimitating the arm. We suggest that the lead-based contrast in this specific case is most probably due to the white lead-based paint lying underneath being spread by the black brush stroke that made the decorative stripes. For PAP-9, the higher amount of lead on one surface is directly correlated to the ink presence (Figure 3A). Finally, PAP-8 is the only fragment for which a chemical contrast was found using iron (Figure 4A), highlighting the presence of the ink on one of the papyrus surfaces. Analysis of the XRD data collected on the ink of the fragments showing lead- and iron-based chemical contrast did not provide additional insights into the possible presence of lead- and iron-based crystalline phases. Only similar phases as the ones found in blank papyrus were identified (Figure 6). A really low content and/or their amorphous nature may explain the lack of sensitivity of the XRD techniques toward the presence of additional lead- and iron-based phases. For more than half of the fragments, the ink seems to be mainly based on flame carbon pigment (in addition to the binder, which is not discussed here), without any additional compound that could have resulted in a chemical contrast with blank papyrus (Table S1). Concerning the samples for which

a chemical contrast was obtained, only one could be compatible with the use of a mixed ink, where a carbon-based pigment is associated with iron salts. Nevertheless, in the present case, the iron-based compound could not be identified, and its presence may also result from nonintentional contamination of the ink during its manufacturing or preparation process. Furthermore, this quasi-absence of iron/copper elements in the carbon-based inks from the Champollion collection is in agreement with the New Kingdom estimation period given by Egyptologists for the largest painted fragments, the use of mixed inks containing copper and iron salts emerging (probably) later in history.<sup>8</sup>

In agreement with former publications on Egyptian papyrus,<sup>9–14</sup> we also report a higher content of lead in the black ink of a few fragments. Our attempt to identify the original lead-based compound being unsuccessful, the question about the intentional addition of such compound or accidental contamination stays open. Egyptians from ancient times had great expertise in manipulating lead-based compounds, with the development of complex chemical processes, for example, resulting in the large-scale production of cosmetics with specific therapeutic properties.<sup>37</sup> Lead compounds are also known to facilitate the drying of oil paintings or varnishes,<sup>38</sup> and the use of litharge (PbO) as drier is reported by Galen as early as the second century AD and by Marcellus (fourth century AD).<sup>16</sup> Due to the advanced knowledge of Ancient Egyptian about lead chemistry, the use of lead compounds to favor the drying of the ink could be a possibility. Nevertheless, artifacts made of lead or lead alloys dating from ancient Egypt have been excavated in several places,<sup>18</sup> and this includes vessels<sup>39</sup> that could have been used to prepare the ink, thus providing a potential source of contamination, as previously discussed by Tack et al.<sup>16</sup> Extracting the Carbon-Based Pigment Contribution of the Ink from the Papyrus Support. Two diffraction patterns collected on the black scepter of god Ra and on the sole papyrus support are displayed in Figure 6A. These

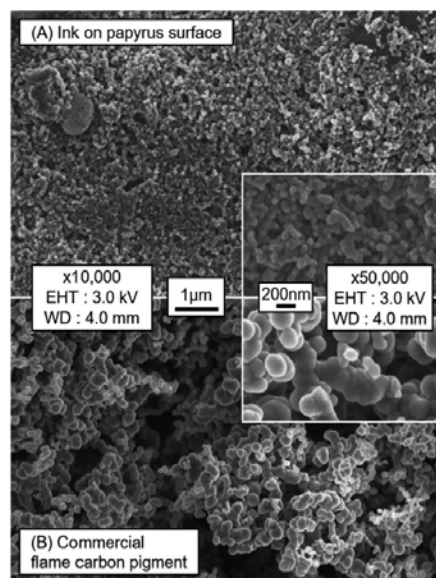


Figure 5. SEM image of (A) black ink at the surface of PAP-2 and (B) commercial flame carbon (“noir de fumée”).

patterns are quite similar to the one collected on blank papyrus (Figure 2B), dominated by the diffraction signal of cellulose, and comparing inked and noninked areas does not show any obvious difference. The diffraction signal of standard flame carbon is also shown, characterized by a large peak over the same Q-range ( $Q = 4\pi \sin(\theta)/\lambda$ ). This absence of structural contrast was expected, first because of the small diffracting volume of flame carbon compared to the volume of papyrus, and because of the main characteristics of both flame carbon and papyrus: they are both made of carbon and have both a quasi-amorphous structure. A way to enhance the sensitivity of diffraction techniques is to use XRD-CT.<sup>27</sup> Such an approach has proven to be efficient to detect phases down to 0.1% in volume<sup>27</sup> and can be applied to the investigation of both crystalline and noncrystalline materials.<sup>28</sup> XRD-CT data were collected on samples PAP-8 and PAP-9, and the reconstructed slices are shown in Figure 3B,E, respectively. Using the overall diffraction signal of the whole fragment did not lead to any contrast between the ink area and the papyrus support (Figure S4). The averaged diffraction signal of the papyrus support was calculated, and, after normalization at high Q-range values, subtracted from the overall diffraction signal. At this point, in both reconstructed slices, a contrast appeared, and the papyrus side on which the ink is apposed was revealed,



for  $Q$  values between 1.15 and 1.64  $\text{\AA}^{-1}$  (Figure 3B,E). The diffraction signal corresponding to the highlighted area on Figure 3B,E was extracted by reverse analysis, and is shown in Figure 3C,F, respectively. The extracted diffraction signal was compared with the diffraction signal of standard flame carbon, and, in both cases, a good match was obtained. This confirms that contrast between the ink and the papyrus support can also be extracted by relying only on the diffraction signal of the carbon-based pigment. To the best of our knowledge, this is the first time that such a pigment-based contrast is revealed. A contrast between ink and papyrus support has also been obtained by XRF-CT, using lead (Figure 3C) and iron (Figure 3A) as discriminating agents, validating the XRD-CT results. Both XRF-CT and XRD-CT results indicate that the ink does not form a distinctive layer at the surface of the papyrus, but has diffused into the papyrus fibers running parallel to the reconstructed slice. Indeed, over a thickness of about 15–20  $\mu\text{m}$ , both papyrus and ink signals are present at the same time. A few additional highlighted spots in the papyrus support can be seen in Figure 3B,D. They do not correspond to the same carbon-based phase identified in the ink, but to additional nonidentified phases with a diffraction contribution at a similar  $Q$  value. We have demonstrated that using an XRD-CT approach, the diffraction signal of the carbon-based pigment used in the ink of ancient papyrus can be extracted and separated from that of the papyrus supports. This may open a new way to investigate ancient and damaged papyrus and use the structural contrast coming from the carbon-based pigment itself in the absence of chemical contrast. In this study, only two slices from two different papyrus fragments of a few hundred micrometers in size were reconstructed. “Reading” of unrolled or damaged papyrus would require scanning of a much larger area and, therefore, adjust our XRD-CT approach to larger volumes. One of the drawbacks of the XRD-CT technique is the measurement time, as the sample is scanned for a series of rotation angles, the spatial resolution being imposed by the size of the beam. From our reconstruction, we have shown that the diffraction signal of the carbon-based pigment is concentrated over the first 15–20  $\mu\text{m}$  inside the papyrus and that the contrast is obtained after carefully subtracting an averaged

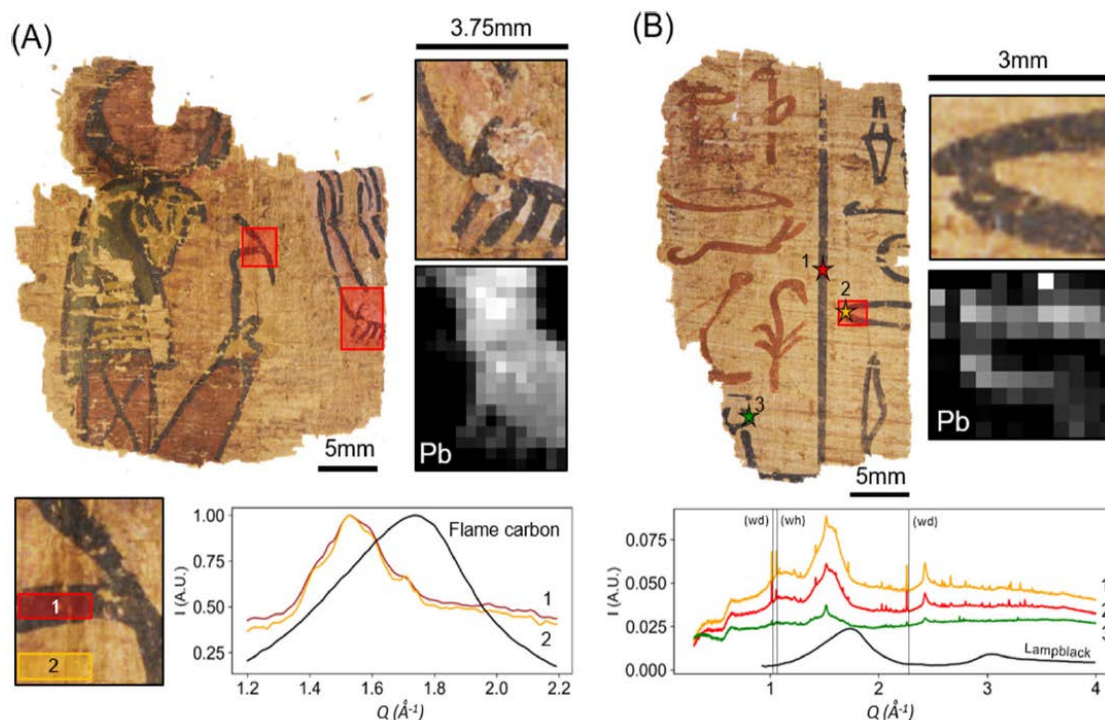


Figure 6. XRD and XRF investigation of PAP-6 and PAP-7. (A) XRF map was retrieved from the deceased’s arm of PAP-6. The lead-based contrast on the four stripes of the garment is most probably related to the presence of lead white used to color the white cloth and the skin. The black scepter region was mapped using XRD, and the average powder diffraction patterns from the inked area and from the papyrus support do not show any significant difference, especially where the main diffraction peak of reference flame carbon is expected. (B) XRF mapping carried out on the “mouth” hieroglyph of PAP-7 shows a lead-based contrast. Three XRD patterns were recorded from three different points of black ink area, the main identified crystalline phases being weddellite (we) and whewellite (wh).

diffraction pattern of the papyrus support to the data. A spatial resolution of about 20  $\mu\text{m}$  should be sufficient to reveal a contrast, thus decreasing the number of scanning steps by a factor of 10 compared to our measurements. Furthermore, several synchrotron sources around the world are undertaking major upgrades,<sup>40,41</sup> and measurements that were taking several hours will be reduced to a few minutes, which could also benefit the Cultural Heritage community.<sup>42</sup> This upgrade would also promote the use of PDF analysis from XRD-CT data, which currently relies on either longer data acquisition or lower statistics. In our case, the possibility to distinguish diverse carbon origins, as demonstrated by Cersoy et al.<sup>43</sup> was not possible. Other diffraction approaches conferring a depth resolution to the measurements could also be a good alternative,<sup>44</sup> as shown by a study from Vanmeert et al. In which the stratigraphy of an illuminated manuscript was reconstructed.<sup>45</sup>

## CONCLUSIONS

The black ink of 10 papyrus fragments coming from the Champollion collection was investigated, combining a series of imaging, spectroscopy, and diffraction techniques. We have shown that the morphology of the papyrus support keeps a trace of the manufacturing process. The carbon-black pigment of the ink was identified as flame carbon, and in a few cases, a chemical contrast between the ink and the papyrus support was retrieved using lead and iron as discriminating agents, the origin of both still being under debate. In addition, we demonstrated that a structural contrast could be obtained solely using the diffraction signal of the carbon-black pigment, thus offering a new possibility to read unrolled or damaged papyrus. Additional insights into the ink manufacturing process would be gained by analyzing a larger selection of samples, and a dedicated methodology should be developed to study the organic binder medium also part of the ink. As suggested by Zerdoun,<sup>3</sup> the type of binder may be the only difference in the preparation of the ink, depending on its use as writing or painting material. Combining several techniques, using both lab- and synchrotron-based sources, we have improved our knowledge of black inks used in ancient Egypt, a further step toward deciphering messages from the past still hidden in Cultural Heritage materials.

## ASSOCIATED CONTENT

\* Supporting Information

The Supporting Information is available free of charge at <https://pubs.acs.org/doi/10.1021/acs.analchem.0c04178>.

Papyrus fragments mounted at ID22; carbon Raman band fitting and width vs D band position; SEM images of peach black and grape black; reverse analysis from the ink areas of PAP-8 and PAP-9 (no subtraction); elemental composition from XRF; position and width of the G and D Raman bands; papyri fragments ownership history; SEM measurements; sample holders for ID22; and XRD-CT/XRF-CT data processing (PDF)

## AUTHOR INFORMATION

Corresponding Authors

Pierre-Olivier Autran – Univ. Grenoble Alpes, CNRS, Grenoble, Institut Néel, Grenoble 38000, France; European Synchrotron Radiation Facility, Grenoble 38000, France; [orcid.org/0000-0003-4600-6371](https://orcid.org/0000-0003-4600-6371); Email: [pierreolivier.autran@esrf.fr](mailto:pierreolivier.autran@esrf.fr)

Pauline Martinetto – Univ. Grenoble Alpes, CNRS, Grenoble, Institut Néel, Grenoble 38000, France; [orcid.org/0000-0003-4093-1822](https://orcid.org/0000-0003-4093-1822); Email: [pauline.martinetto@neel.cnrs.fr](mailto:pauline.martinetto@neel.cnrs.fr)

Authors

Catherine Dejoie – European Synchrotron Radiation Facility,  
Grenoble 38000, France

Pierre Bordet – Univ. Grenoble Alpes, CNRS, Grenoble,  
Institut Néel, Grenoble 38000, France;  
[orcid.org/0000-0002-1488-2257](https://orcid.org/0000-0002-1488-2257)

Jean-Louis Hodeau – Univ. Grenoble Alpes, CNRS, Grenoble,  
Institut Néel, Grenoble 38000, France

Caroline Dugand – Département de l'Isère, Musée  
Champollion, Vif 38450, France

Maeva Gervason – Département de l'Isère, Musée  
Champollion, Vif 38450, France

Michel Anne – Univ. Grenoble Alpes, CNRS, Grenoble,  
Institut Néel, Grenoble 38000, France

#### Author Contributions

The manuscript was written through contributions of all authors.

#### Notes

The authors declare no competing financial interest.

#### ACKNOWLEDGMENTS

The authors would like to thank Valérie Reita and Sébastien Pairis (Institut Néel CNRS Grenoble, France) for their help in the manipulation of the Raman spectrometers and the scanning electron microscope, respectively. They also thank Dr. J. P. Wright and Dr. A. N. Fitch (ESRF Grenoble, France) for their help during the experiments at the ID11 and the ID22 beamlines and for their kind advice. P.O.A. acknowledges the ESRF and the Néel Institute for his Ph.D. studentship.

#### REFERENCES

- (1) Lucas, A.; Harris, J. R. *Ancient Egyptian Materials and Industries*, 4. ed., rev.enl.; Histories & Mysteries of Man: London, 1989.
- (2) Mond, R.; Myers, O. H.. *Cemeteries of Armant, I*; The Egypt Exploration Society, Milford, H., Oxford University Press: London, 1937.
- (3) Zerdoun, B.-Y. M.. *Les Encre Noires Au Moyen Age (Jusqu'à 1600)*; Documents, études et répertoires; Editions du Centre national de la recherche scientifique: Paris, 1983.
- (4) Garlan, Y. *Recherches de Poliorcétique Grecque*, Bibliothèque Des Ecoles Françaises d'Athènes et de Rome. Paris: Bibliothèque des Ecoles Françaises d'Athènes et de Rome 1974, 324.
- (5) Osbaldeston, T. A. *Dioscorides de Materia Medica*; Ibidis: Johannesburg, 2000.
- (6) Bostock, J.; Riley, H. T.. *Pliny the Elder: The Natural History*; 1855; XXXV, 25.
- (7) Pollio, V.. *Ten books on architecture*; Rowland, I. D., Howe, T. N., Eds.; Cambridge University Press: Cambridge, 1999; VII, 10.
- (8) Colini, C.; Hahn, O.; Bonnerot, O.; Steger, S.; Cohen, Z.; Ghigo, T.; Christiansen, T.; Bicchieri, M.; Biocca, P.; Krutzsch, M.; Rabin, I. *The Quest for the Mixed Inks*. 2018.
- (9) Arlt, T.; Mahnke, H.-E.; Siopi, T.; Menei, E.; Aibe' o, C.; Pausewein, R.-R.; Reiche, I.; Manke, I.; Lepper, V. J. *Cult. Herit.* 2019, 39, 13–20.
- (10) Mocella, V.; Brun, E.; Ferrero, C.; Delattre, D. *Nat. Commun.* 2015, 6, 5895.
- (11) Christiansen, T.; Cotte, M.; Loredó-Portales, R.; Lindelof, P. E.; Mortensen, K.; Ryholt, K.; Larsen, S. *Sci. Rep.* 2017, 7, 15346.
- (12) Gore, D. B.; Choat, M.; Jacob, D. E.; Gloy, G. *Powder Diffr.* 2017, 32, S90–S94.
- (13) Ghigo, T.; Rabin, I.; Buzi, P. *Archaeol. Anthropol. Sci.* 2020, 12, 70.

- (14) Brun, E.; Cotte, M.; Wright, J.; Ruat, M.; Tack, P.; Vincze, L.; Ferrero, C.; Delattre, D.; Mocella, V. *Proc. Natl. Acad. Sci. U. S. A.* 2016, 113, 3751–3754.
- (15) Christiansen, T.; Buti, D.; Dalby, K. N.; Lindelof, P. E.; Ryholt, K.; Vila, A. J. *Archaeol. Sci. Rep.* 2017, 14, 208–219.
- (16) Tack, P.; Cotte, M.; Bauters, S.; Brun, E.; Banerjee, D.; Bras, W.; Ferrero, C.; Delattre, D.; Mocella, V.; Vincze, L. *Sci. Rep.* 2016, 6, 20763.
- (17) Delange, E.; Grange, M.; Kusko, B.; Menei, E. *Revue d'Égyptologie* 1990, 213–217.
- (18) *Ancient Egyptian Materials and Technology*, 1. Aufl.; 5. Neudr.; Nicholson, P. T.; Shaw, I., Eds.; Cambridge Univ. Pr: Cambridge, 2009.
- (19) Winter, J. *Stud. Conserv.* 1983, 28, 49–66.
- (20) Burgio, L.; Clark, R. J. H. *J. Raman Spectrosc.* 2000, 31, 395–401.
- (21) Tomasini, E. P.; Halac, E. B.; Reinoso, M.; Di Liscia, E. J.; Maier, M. S. *J. Raman Spectrosc.* 2012, 43, 1671–1675.
- (22) Wiedeman, H. G.; Bayer, G. *Anal. Chem.* 1983, 55, 1220A–1230A.
- (23) Parker, C. S.; Parsons, S.; Bandy, J.; Chapman, C.; Coppens, F.; Seales, W. B. *PLoS One* 2019, 14, No. e0215775.
- (24) Ashiotis, G.; Deschildre, A.; Nawaz, Z.; Wright, J. P.; Karkoulis, D.; Picca, F. E.; Kieffer, J. J. *Appl. Crystallogr.* 2015, 48, 510–519.
- (25) Coelho, A. A. J. *Appl. Crystallogr.* 2018, 51, 210–218.
- (26) Sole, V. A.; Papillon, E.; Cotte, M.; Walter, P.; Susini, J. *Spectrochim. Acta Part B: Atom. Spectrosc.* 2007, 62, 63–68.
- (27) Bleuët, P.; Welcomme, E.; Dooryhe, E.; Susini, J.; Hodeau, J.-L.; Walter, P. *Nat. Mater.* 2008, 7, 468–472.
- (28) Alvarez-Murga, M.; Bleuët, P.; Hodeau, J.-L. *J. Appl. Crystallogr.* 2012, 45, 1109–1124.
- (29) Wallert, A. *Stud. Conserv.* 1989, 34, 1–8.
- (30) Gaudet, J. J. *Ecol.* 1975, 63, 483.
- (31) Gates-Rector, S.; Blanton, T. *Powder Diffr.* 2019, 34, 352–360.
- (32) Jawhari, T.; Roid, A.; Casado, J. *Carbon* 1995, 33, 1561–1565.
- (33) Mernagh, T. P.; Cooney, R. P.; Johnson, R. A. *Carbon* 1984, 22, 39–42.
- (34) Coccato, A.; Jehlicka, J.; Moens, L.; Vandenberghe, P. J. *J. Raman Spectrosc.* 2015, 46, 1003–1015.
- (35) Goler, S.; Yardley, J. T.; Cacciola, A.; Hagadorn, A.; Ratzan, D.; Bagnall, R. J. *J. Raman Spectrosc.* 2016, 47, 1185–1193.
- (36) Tomasini, E.; Siracusano, G.; Maier, M. S. *Microchem. J.* 2012, 102, 28–37.
- (37) Walter, P.; Martinetto, P.; Tsoucaris, G.; Brniaux, R.; Lefebvre, M. A.; Richard, G.; Talabot, J.; Dooryhe, E. *Nature* 1999, 397, 483–484.
- (38) Tumosa, C. S.; Mecklenburg, M. F. *Stud. Conserv.* 2005, 50, 39–47.
- (39) Petrie, W. M. F. *Objects of Daily Use; The Petrie Egyptian Collection and Excavations*; Aris & Phillips [u.a.]: Warmister, Wiltshire, 1974.
- (40) Raimondi, P. *Synchrotr. Radiat. News* 2016, 29, 8–15.
- (41) Sajaev, V. *Phys. Rev. Accel. Beams* 2019, 22, No. 040102.
- (42) Cotte, M.; Autran, P.-O.; Berruyer, C.; Dejoie, C.; Susini, J.; Tafforeau, P. *Synchrotr. Radiat. News* 2019, 32, 34–40.
- (43) Cersoy, S.; Martinetto, P.; Bordet, P.; Hodeau, J. L.; Van Elslande, E.; Walter, P. J. *Appl. Crystallogr.* 2016, 49, 585–593.
- (44) Dejoie, C.; Coduri, M.; Petitdemange, S.; Giacobbe, C.; Covacci, E.; Grimaldi, O.; Autran, P.-O.; Mogodi, M. W.; S'ak Jung, D.; Fitch, A. N. *J. Appl. Crystallogr.* 2018, 51, 1721–1733.